Supporting Information

Rationally Designed Trimetallic Prussian Blue Analogue on LDH/Ni Foam for High Performance Supercapacitor

Chen Chen,[a] Shi-Cheng Wang,[a] Dengke Xiong,[a] Minli Gu[a] and Fei-Yan Yi[a,b,c]*

[a] School of Materials Science & Chemicals Engineering, Ningbo University, Ningbo, Zhejiang 315211, China. E-mail:yifeiyan@nbu.edu.cn

[b] State Key Laboratory of Structure Chemistry, Fujian Institute of Research on the Structure of Matter, Chinese Academy of Sciences, Fuzhou 350002, P. R. China.

[c] Key Laboratory of Photoelectric Detection Materials and Devices of Zhejiang Province, Ningbo University, Ningbo, 315211, China

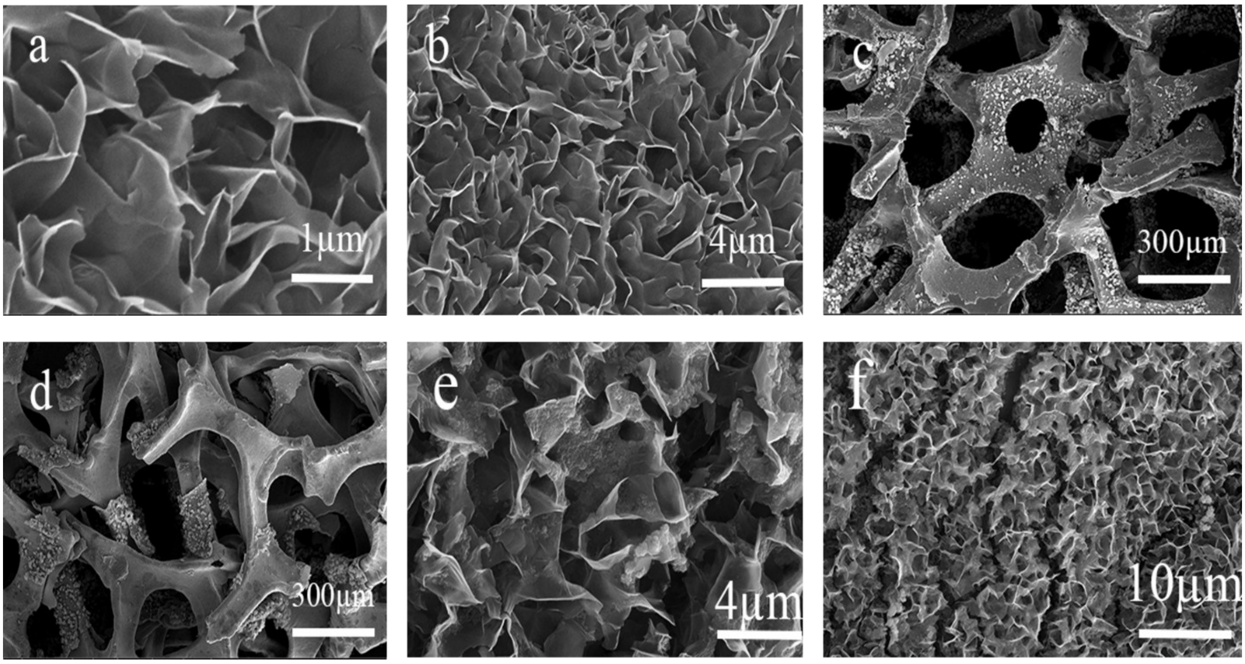

Fig. S1 SEM images of NiCo-LDH/NF nanosheets (a-c), PBA@NiCo-LDH/NF (d) at 180ºC and PBA@NiCo-LDH nanocomposites (e-f) at 120ºC.

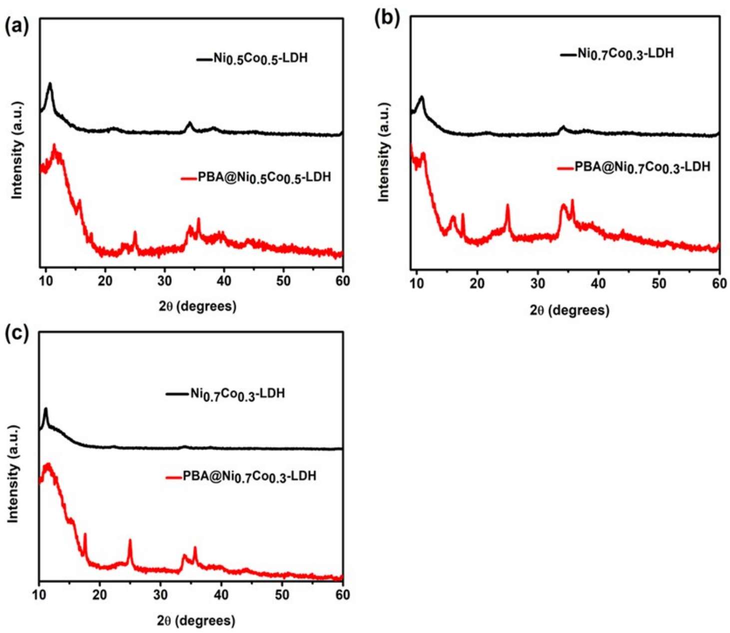

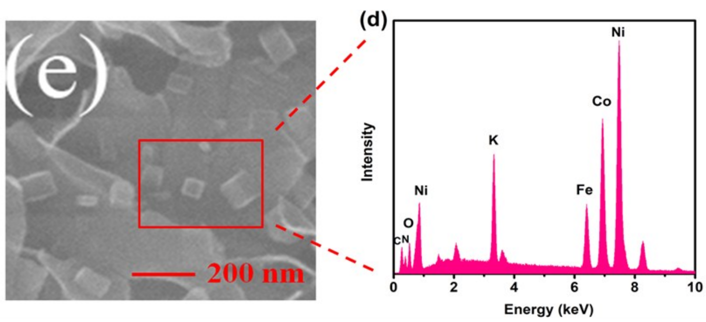

Fig. S2 XRD patterns of $Ni_{0.5}Co_{0.5}$-LDH and PBA@$Ni_{0.5}Co_{0.5}$-LDH powders (a); $Ni_{0.7}Co_{0.3}$-LDH and PBA@$Ni_{0.7}Co_{0.3}$-LDH powders (b,120 ºC); $Ni_{0.7}Co_{0.3}$-LDH and PBA@$Ni_{0.7}Co_{0.3}$-LDH powder (c,180 ºC); (d and e) EDS for PBA nanoparticles on the surface of PBA@$Ni_{0.4}Co_{0.6}$-LDH/NF.

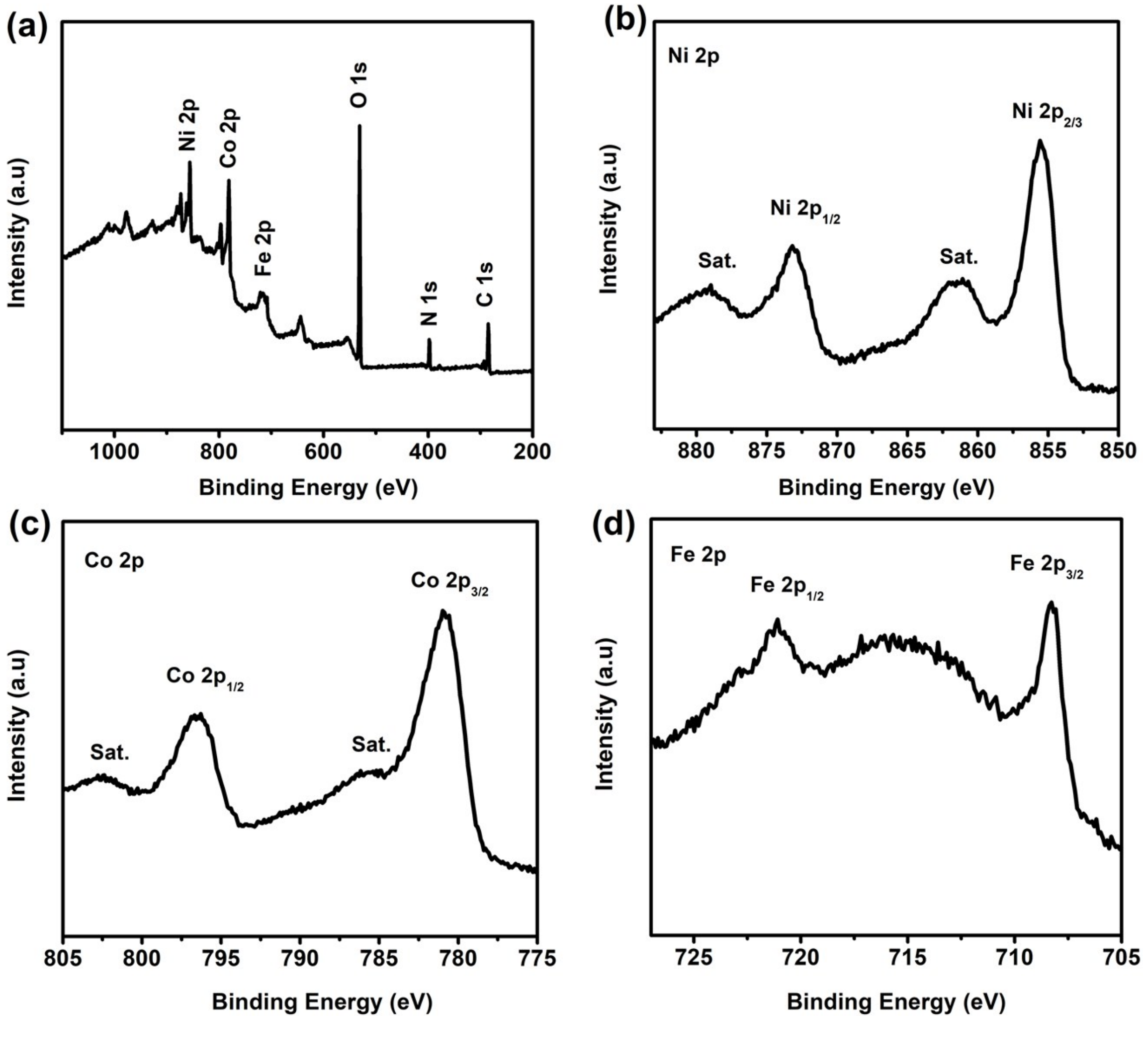

Fig. S3 XPS spectra for (a) PBA@$Ni_{0.4}Co_{0.6}$-LDH; (b) Ni 2p, (c) Co 2p, (d) Fe 2p

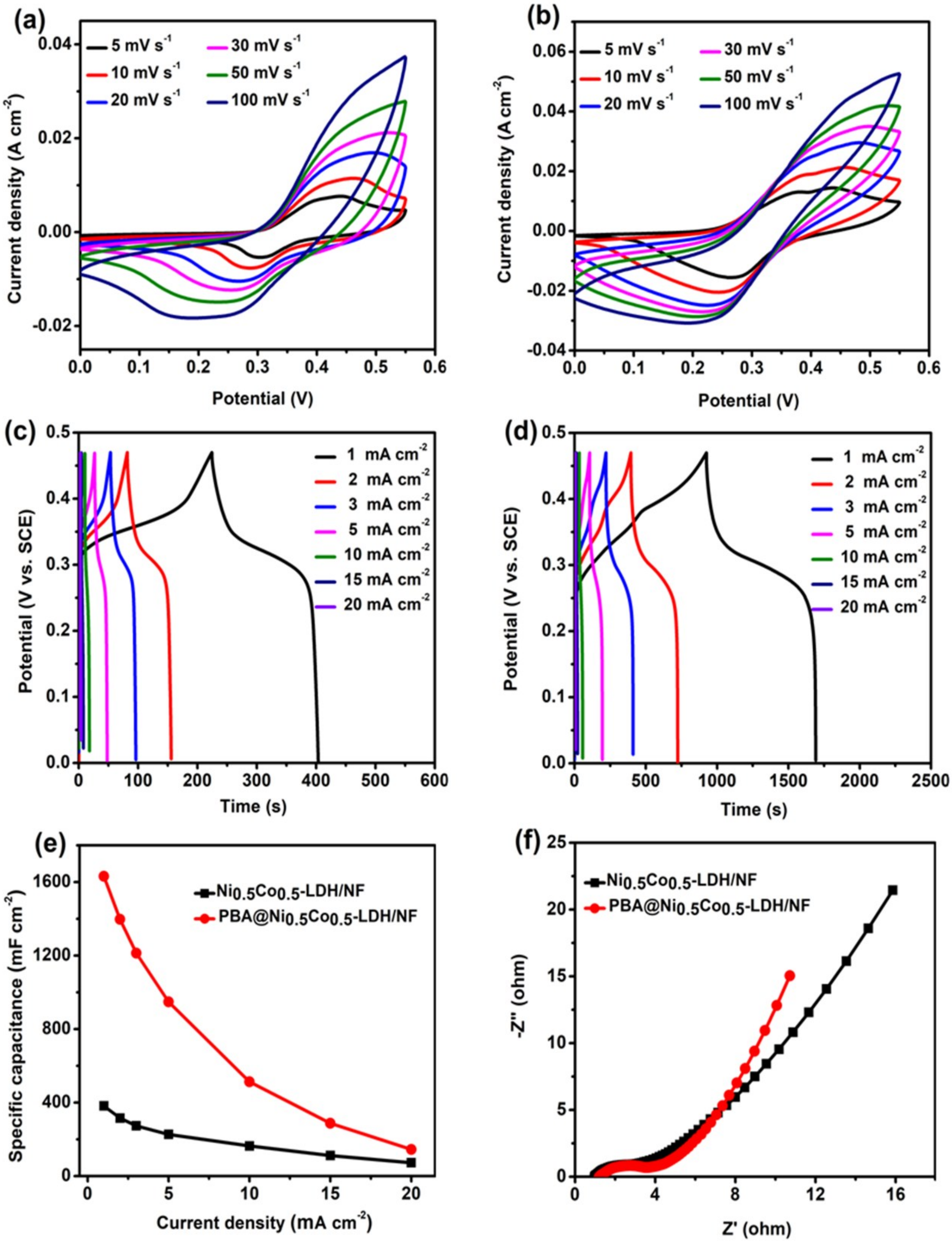

Fig. S4 CV of $Ni_{0.5}Co_{0.5}$-LDH/NF (a) and PBA@$Ni_{0.5}Co_{0.5}$-LDH/NF (b); GCD test of $Ni_{0.5}Co_{0.5}$-LDH/NF (c) and PBA@$Ni_{0.5}Co_{0.5}$-LDH/NF (d); specific capacitance and density curves of $Ni_{0.5}Co_{0.5}$-LDH/NF and PBA@$Ni_{0.5}Co_{0.5}$-LDH/NF (e); EIS test of $Ni_{0.5}Co_{0.5}$-LDH/NF and PBA@$Ni_{0.5}Co_{0.5}$-LDH/NF (f).

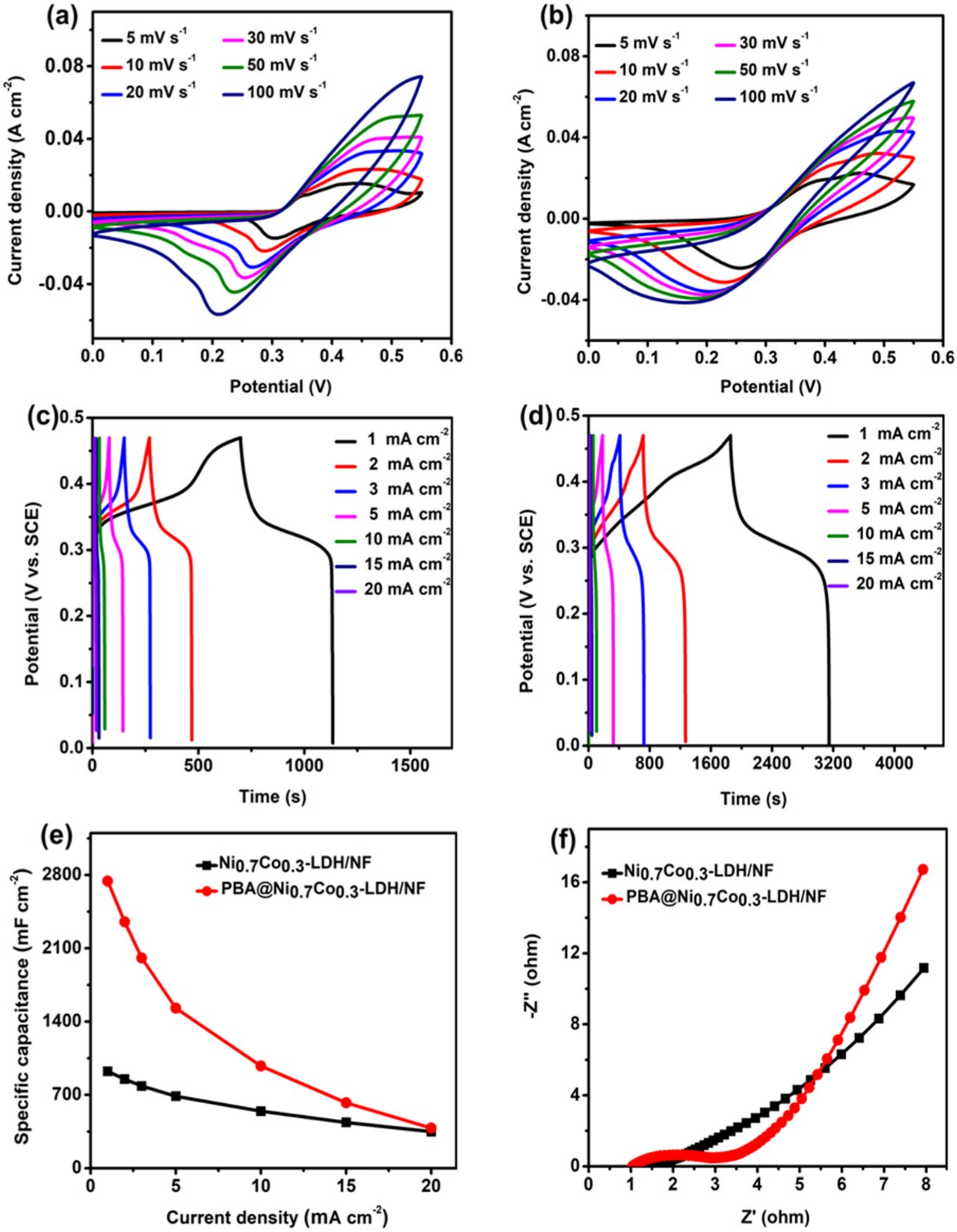

Fig. S5 CV of $Ni_{0.7}Co_{0.3}$-LDH/NF (a) and PBA@$Ni_{0.7}Co_{0.3}$-LDH/NF (b); GCD test of $Ni_{0.7}Co_{0.3}$-LDH/NF (c) and PBA@$Ni_{0.7}Co_{0.3}$-LDH/NF (d); specific capacitance and density curves of $Ni_{0.7}Co_{0.3}$-LDH/NF and PBA@$Ni_{0.7}Co_{0.3}$-LDH/NF (e); EIS test of $Ni_{0.7}Co_{0.3}$-LDH/NF and PBA@$Ni_{0.7}Co_{0.3}$-LDH/NF (f).

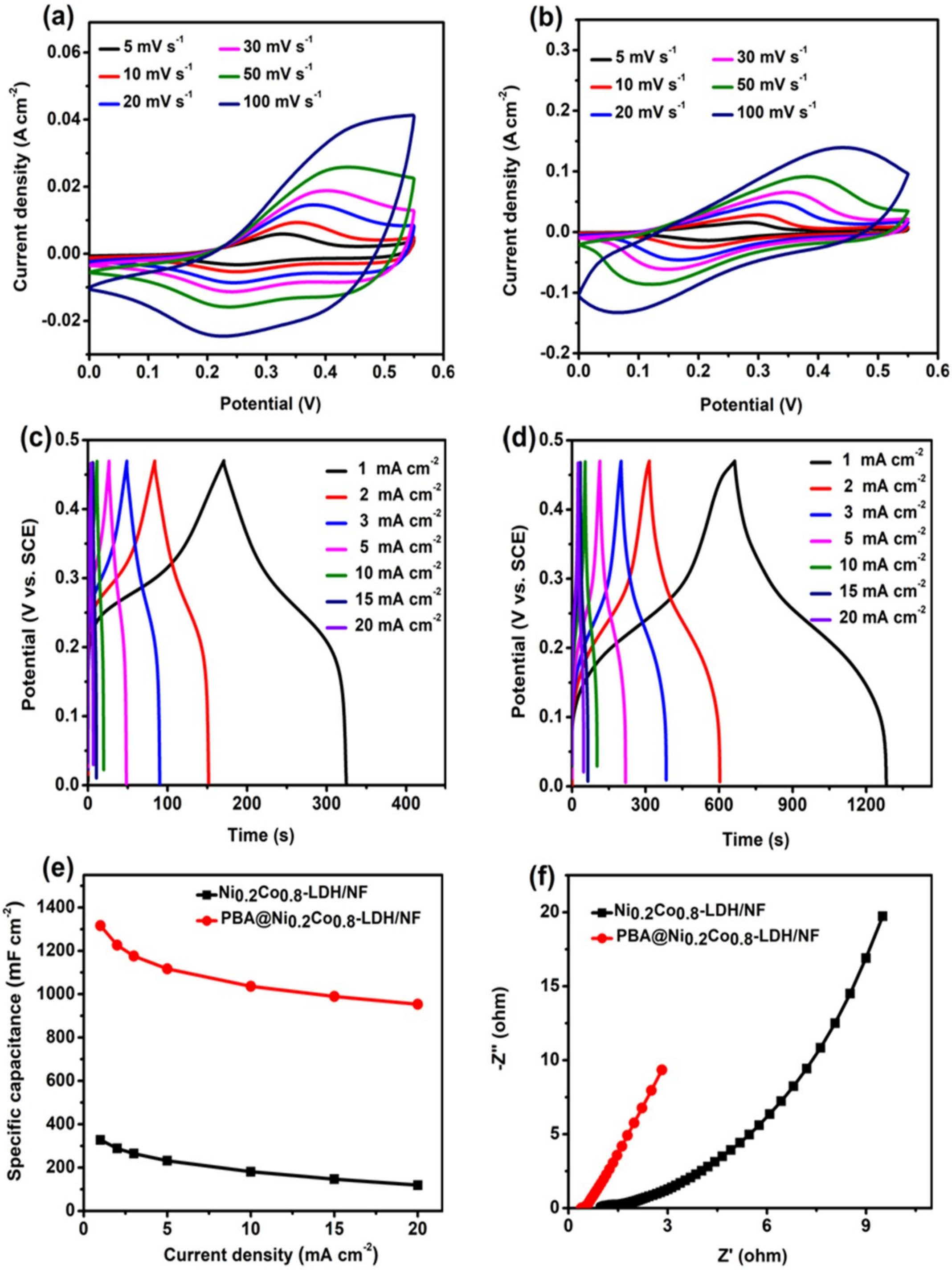

Fig. S6 CV of $Ni_{0.2}Co_{0.8}$-LDH/NF (a) and PBA@$Ni_{0.2}Co_{0.8}$-LDH/NF (b); GCD test of $Ni_{0.2}Co_{0.8}$-LDH/NF (c) and PBA@$Ni_{0.2}Co_{0.8}$-LDH/NF (d); specific capacitance and density curves of $Ni_{0.2}Co_{0.8}$-LDH/NF and PBA@$Ni_{0.2}Co_{0.8}$-LDH/NF (e); and EIS test of $Ni_{0.2}Co_{0.8}$-LDH/NF and PBA@$Ni_{0.2}Co_{0.8}$-LDH/NF (f).

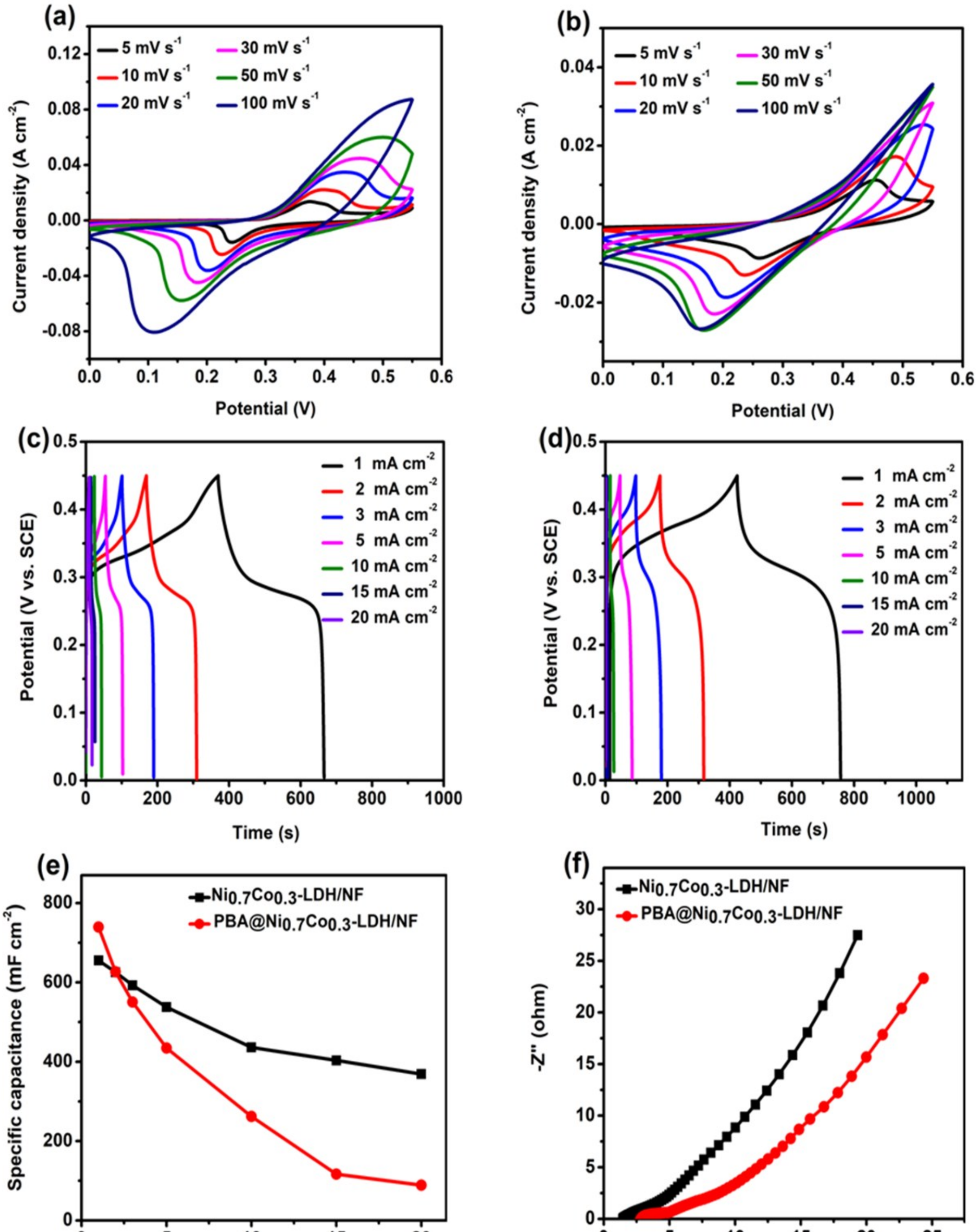

Fig. S7 At 180ºC, CV of $Ni_{0.7}Co_{0.3}$-LDH/NF (a) and PBA@$Ni_{0.7}Co_{0.3}$-LDH/NF (b); GCD test of $Ni_{0.7}Co_{0.3}$-LDH/NF (c) and PBA@$Ni_{0.7}Co_{0.3}$-LDH/NF (d); specific capacitance and density curves of $Ni_{0.7}Co_{0.3}$-LDH/NF and PBA@$Ni_{0.7}Co_{0.3}$-LDH/NF (e); EIS test of $Ni_{0.7}Co_{0.3}$-LDH/NF and PBA@$Ni_{0.7}Co_{0.3}$-LDH/NF (f).

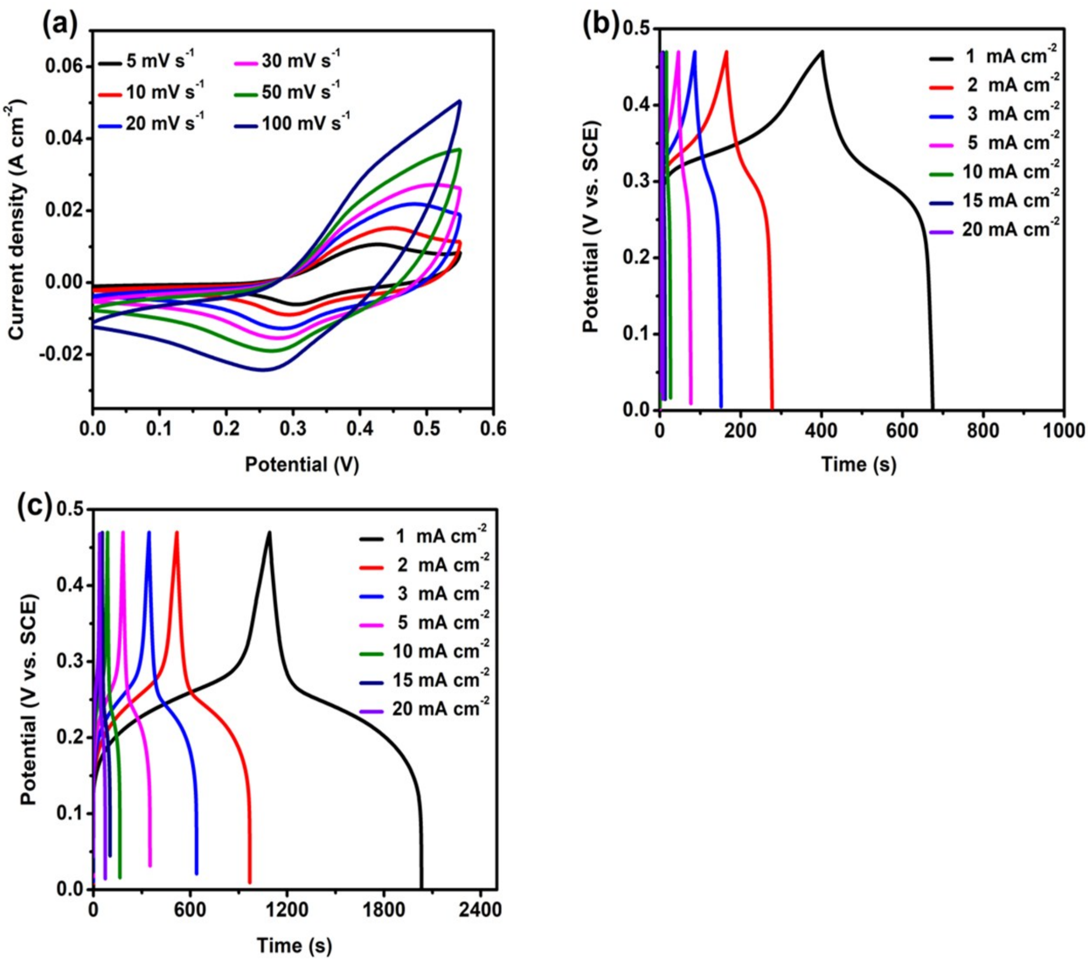

Fig. S8 CV of $Ni_{0.4}Co_{0.6}$-LDH/NF (a); GCD test of $Ni_{0.4}Co_{0.6}$-LDH/NF (b) and PBA@$Ni_{0.4}Co_{0.6}$-LDH/NF (c).

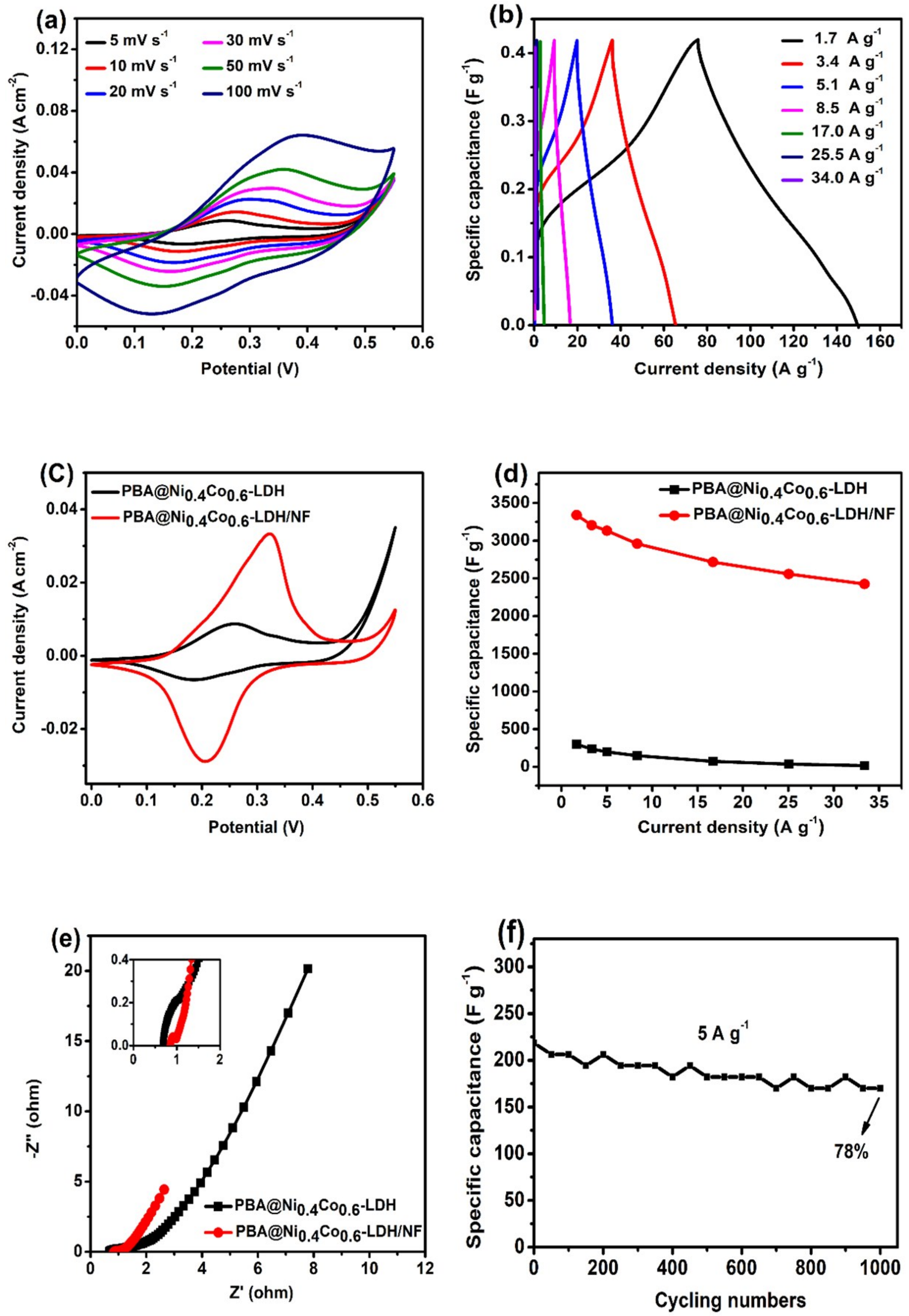

Fig. S9 (a) CV of PBA@$Ni_{0.4}Co_{0.6}$-LDH; (b) GCD test of PBA@$Ni_{0.4}Co_{0.6}$-LDH; (c) CV of PBA@$Ni_{0.4}Co_{0.6}$-LDH and PBA@$Ni_{0.4}Co_{0.6}$-LDH/NF at 5 mV s^{-1}; (d) specific capacitance and density curves of PBA@$Ni_{0.4}Co_{0.6}$-LDH and PBA@$Ni_{0.4}Co_{0.6}$-LDH/NF; (e) EIS test of PBA@$Ni_{0.4}Co_{0.6}$-LDH and PBA@$Ni_{0.4}Co_{0.6}$-LDH/NF; (f) cyclic performance of PBA@$Ni_{0.4}Co_{0.6}$-LDH and PBA@$Ni_{0.4}Co_{0.6}$-LDH/NF.

The electrochemical performance of PBA@$Ni_{0.4}Co_{0.6}$-LDH was tested under the similar condition as PBA@$Ni_{0.4}Co_{0.6}$-LDH/NF. As shown in Fig. S9a, it can be observed that the anodic and cathodic peaks move towards positive potential and negative potential, respectively, as the scan rate increases from 5 to 100 mV s^{-1}, demonstrating the quasi-reversible redox processes. Fig. S9c shows clearly that the PBA@$Ni_{0.4}Co_{0.6}$-LDH/NF displays larger integral area and higher current density than PBA@$Ni_{0.4}Co_{0.6}$-LDH. To compare their capacitive properties, the GCD test was conducted at the same current density. It can be observed that the voltage window did not reach 0.47 V for PBA@$Ni_{0.4}Co_{0.6}$-LDH during GCD test, thus the voltage window was set to 0.42 V. The capacitive performance for PBA@$Ni_{0.4}Co_{0.6}$-LDH/NF is also obviously superior to corresponding PBA@$Ni_{0.4}Co_{0.6}$-LDH (Fig. S9b, d). In addition, EIS results (Fig. S9e) show that the semicircle radius of PBA@$Ni_{0.4}Co_{0.6}$-LDH/NF in the high-frequency region is significantly smaller than PBA@$Ni_{0.4}Co_{0.6}$-LDH. PBA@$Ni_{0.4}Co_{0.6}$-LDH exhibits similar stability as PBA@$Ni_{0.4}Co_{0.6}$-LDH/NF based on result of 1000 cycles of charge-discharge test(Fig. S9f).

All of electrochemical properties fully demonstrate that PBA@$Ni_{0.4}Co_{0.6}$-LDH/NF displays much better electrochemical performance than corresponding PBA@$Ni_{0.4}Co_{0.6}$-LDH, as the growth of PBA@$Ni_{0.4}Co_{0.6}$-LDH nanocomposite on Ni foam can significantly improve its electrical conductivity.

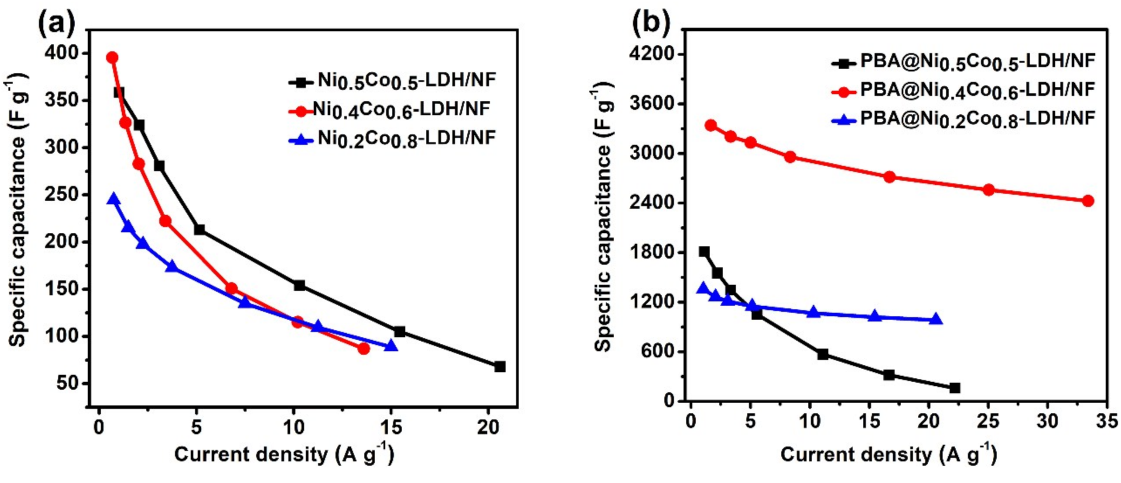

Fig. S10 Specific capacitance and density curves of Ni_xCo_{1-x}-LDH/NF (a) and PBA@Ni_xCo_{1-x}-LDH/NF (b).

During the synthetic process for PBA@NiCo-LDH/NF nanocomposites, the Ni foam with same weight and size is used, the total amount of $Co(NO_3)_2 \cdot 6H_2O$ and $Ni(NO_3)_2 \cdot 6H_2O$ is kept to 2 mmol, as well as $K_3[Fe(CN)_6]$ solution with same volume and concentration (2 mmol, 10 mL) was used to to synthesize all of NiCo-LDH/NF and PBA@NiCo-LDH/NF materials. Therefore, the mass of each nanocomposite can be controlled very well. In addition, each material was weighed before testing the electrochemical property and their weight is similar to each other. Therefore, in this work, both of them are reasonable for the area specific capacitance and gravimetric specific capacitance.”

In fact, as depicted in Fig. S10, the gravimetric specific capacitance of PBA@$Ni_{0.4}Co_{0.6}$-LDH/NF is higher than the result from area specific capacitance (Fig. 3). However, to express more accurately the capacitance result of each material, the area specific capacitance was adopted finally in this work, since the area of Ni foam can be kept very well and same, a very slight difference in the mass of material can be observed before and after tests, which may be caused by droping out of PBA nanoparticles.

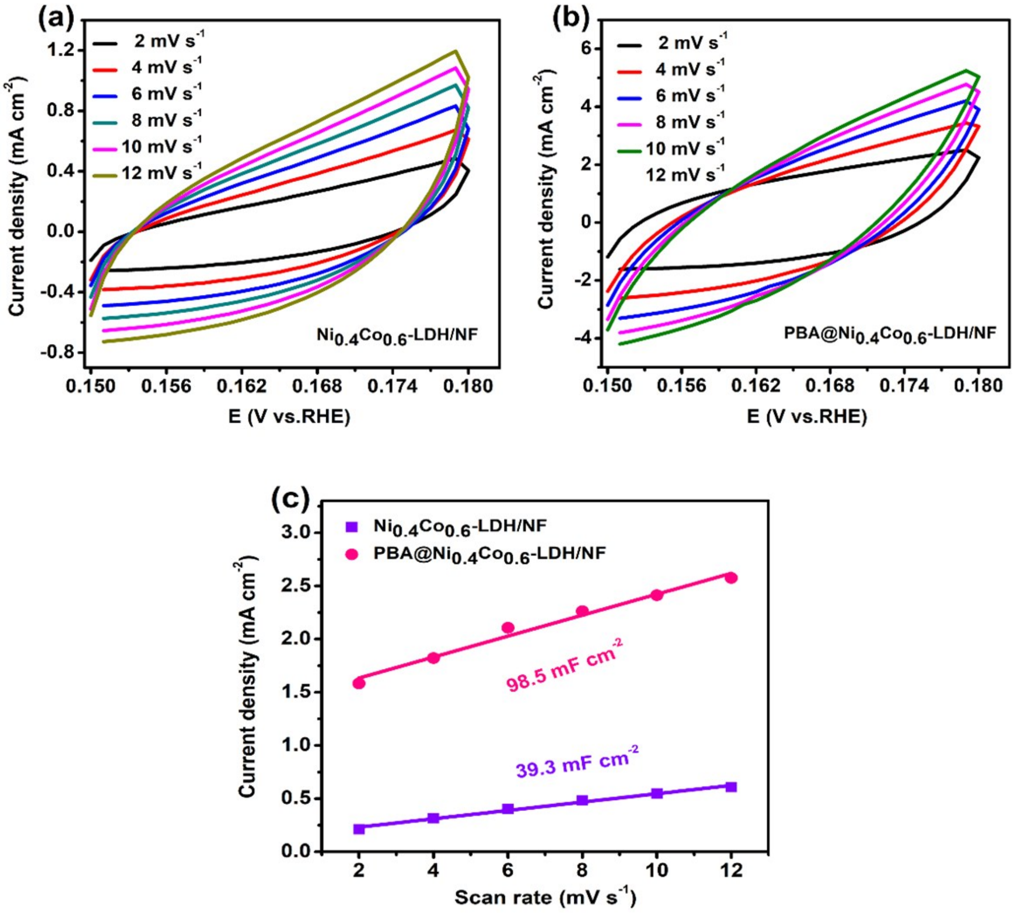

Fig. S11 CV curves of $Ni_{0.4}Co_{0.6}$-LDH/NF (a) and PBA@$Ni_{0.4}Co_{0.6}$-LDH/NF (b) without redox region at scan rates of 2, 4, 6, 8, 10, 12 mV s^{-1}; (c) the capacitive currents as a function of scan rate for $Ni_{0.4}Co_{0.6}$-LDH/NF and PBA@$Ni_{0.4}Co_{0.6}$-LDH/NF.

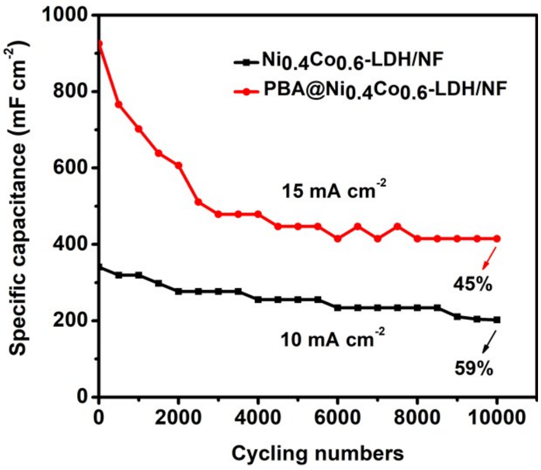

Fig. S12 Cyclic performance of $Ni_{0.4}Co_{0.6}$-LDH/NF and PBA@$Ni_{0.4}Co_{0.6}$-LDH/NF at 10 mA cm^{-2} and 15 mA cm^{-2}, respectively.